760 *J. Phys. Chem. A* **2002,** *106,* 760−766

Self-Modeling Curve Resolution Study of Temperature-Dependent Near-Infrared Spectra of Water and the Investigation of Water Structure

S. Šašić,[†] V. H. Segtnan,[†,‡] and Y. Ozaki*[,†]

Department of Chemistry, School of Science, Kwansei-Gakuin University, Gakuen, Sanda, Hyogo 669-1337, Japan, and Department of Food Science, Agricultural University of Norway, N-1432 Ås, Norway

Received: September 7, 2001

A self-modeling curve resolution method called Simplisma is used to investigate the 1300−1600 nm near-infrared region of the water spectrum. The most specific wavelengths of the analytes present are identified through the ratios of the standard deviations to the means of spectroscopic variations for all of the wavelengths. Without any prior knowledge about the system or supplementary experimental data, we demonstrate that only two species are enough to represent more than 99% of the original data with at least one additional spectroscopically identifiable component. The features of the species and their concentration profiles are calculated. The results are discussed in light of several previous spectroscopic and theoretical studies of water. It is found that a quasi-lattice model with broken hydrogen bonds is highly supported by the present study.

Introduction

The investigations of the structure of water date back nearly a century. Many models have been proposed upon the basis of experimental studies and theoretical calculations.[1,2] These models are divided into two major groups: (1) water is a mixture of two or more components and (2) water is a continuum system in which hydrogen bonds are continuously weakened with increasing temperature. The former is considered to be composed of discrete species that differ according to their structural arrangements. The latter is a network of tetrahedrally bonded water molecules with continuous distribution of intermolecular interactions.[1,2] Vibrational spectroscopy has been employed extensively to support one of these two global models.[3−23] The overall spectroscopic results arguably show that water structure is somewhere between the above two definitions, definitely closer to the two-component model in terms of the formal spectral analysis. However, the continuous model better describes the nature of water's hydrogen bonding, which is the most important factor responsible for spectral dynamics.

Among vibrational spectroscopy techniques, Raman spectroscopy has been most widely exploited because of its suitability for measuring water systems,[10−13,17,21,22] while near-infrared (NIR) and infrared techniques have been used somewhat less. NIR spectra of water are usually measured in the region of 1.3−1.8 μm where bands due to combinations and overtone modes of H_2O appear.[4,9,19] The main purpose of the spectral studies is identification of spectroscopically active species, as well as their quantification. The positions, intensities, bandwidths, and dynamics of the bands identified serve to postulate the nature of the species. Despite the simple structural formula of the water molecule, the vibrational spectra of water consist of several severely overlapping bands and have generated much attention. To date, despite of careful experimental and computational analyses, there are still some challenging questions.

The spectra have been analyzed mainly through the spectral variables (wavelengths or wavenumbers) that were designated for each specific species.[4,19] Such an approach is known in analytical spectroscopy as "univariate calibration" and is strongly based on the fact that there exists at least one unique spectral variable for each of the species of which the intensity changes are caused by exclusively one of species. The finding of these particular variables is, however, strongly hindered by bands overlapping; as the overlap gets higher, the identification of the univariate points becomes harder. The problem has usually been overcome by diluting H_2O in D_2O, which yields sharpening of band structure due to uncoupling of fundamental stretching motions.[4,5,19,22] It has been suggested that this method also helps to assign the bands. Though the relationship between the peaks used as univariate points and the species that are known as "hydrogen-bonded" (HB) (species that dominate at the lower temperatures) and non-hydrogen-bonded (NHB) (species of which the hydrogen bonds are stretched or bent but not literally broken) seems to be justified, the visual impression that these peaks could be univariate points is not entirely convincing, at least for most of the spectral studies using NIR spectra. Besides univariability, another problem for unravelling water spectra lies in the decomposition of the spectra by means of commercial software packages for deconvolution.[13] These routines bear some subjectivity that should be avoided whenever possible. To avoid these problems NIR spectra of pure water could be examined using a multivariate self-modeling curve resolution (SMCR) approach.

NIR spectroscopy has several advantages over Raman and IR spectroscopy for the spectral analysis of water that we employ here: (1) Water adsorption in the IR region is so strong that the spectra of each species are almost indistinguishable. (2) The signal-to-noise ratio of Raman spectra of water may be insufficient for successful application of SMCR methods. (3) When one measures an IR spectrum of water, one must use a very thin cell or an attenuated total reflection (ATR) cell. Thus, one always suffers from the problem of adsorption of water to the cell wall. (4) NIR spectroscopy is concerned with overtones

---

* To whom correspondence should be addressed. Fax: +81-795-65-9077. E-mail: ozaki@kwansei.ac.jp.

[†] Kwansei-Gakuin University.

[‡] Agricultural University of Norway.

10.1021/jp013436p CCC: $22.00

and combination tones so that the separation of bands of each species is better in the NIR.

There are several techniques in the field of analytical spectroscopy that can be entitled as SMCR methods. We use the "Simplisma" method proposed by Windig et al.,[24-26] which is strongly based on the linear algebra representation of the spectral data. Simplisma searches for possible univariate points investigating all of the spectral variables. The technique is unbiased, reasonably simple, and efficient. To the best of our knowledge, there is only one SMCR study of the IR spectra of water in which the pure component spectra, concentration profiles, and enthalpy change of the breaking of one hydrogen bond were calculated by a method called sequential rank analysis.[27] The results of this study were subsequently used by the same authors to deconvolute the NIR spectra of water in the 9000−4200 cm^{-1} region.[28] The aim of this study is to decompose temperature-dependent NIR spectra of water by use of an advanced curve resolution technique, to identify the number of species present, to calculate their concentration profiles, and to estimate (if possible) the enthalpy change (ΔH) of the reaction of breaking one hydrogen bond. Furthermore, with the use of the obtained results, the proposed models of water structure are discussed.

Method of Data Analysis

We offer a brief description of Simplisma. Should the reader want a more in-depth treatment, we recommend refs 24−26. If the spectra are aligned in rows forming a matrix, **X**, and if Beer's law holds in the range of experimental conditions, then **X** can be approximated as

$$\mathbf{X} = \mathbf{C}\mathbf{S}^{\mathrm{T}} + \mathbf{E} \tag{1}$$

where columns of **C** are concentration profiles of the pure components, rows of $\mathbf{S}^{\mathrm{T}}$ are pure component spectra, and **E** is a matrix that contains the errors of approximation. If we know the variables (wavelengths or wavenumbers) at which each of the species solely absorbs with no interferences of other species (i.e., pure variables), then pure component spectra can be calculated by

$$\mathbf{S}^{\mathrm{T}} = (\mathbf{C}^{\mathrm{T}}\mathbf{C})^{-1}\mathbf{C}^{\mathrm{T}}\mathbf{X} \tag{2}$$

because the columns of **C** can be approximated by the absorbance variations along the pure variables. If we know which samples contain the pure component spectra, then pure concentrations can be obtained as

$$\mathbf{C} = \mathbf{X}\mathbf{S}(\mathbf{S}^{\mathrm{T}}\mathbf{S})^{-1} \tag{3}$$

However, the definition of pure variables and pure samples is seriously hampered with increasing spectral overlap.

Simplisma defines pure variables as those having the highest ratio of standard deviations to corresponding means. If the linear algebra is applicable (Beer's law is valid), then the intensity changes along every variable can be viewed as vectors with those at the pure variables being orthogonal axes that are geometry extremes in the multivariate space of data. All other intensity changes can be obtained by the linear combinations of these orthogonal vectors. The general characteristic of these vectors is that they show the highest ratio

$$\frac{\delta_j}{d_j} \tag{4}$$

where δ_j is the standard deviation of the j-th variable defined as

$$\delta_j = \sqrt{\frac{1}{n_{\mathrm{spec}}}\sum_{i=1}^{n_{\mathrm{spec}}}(d_{ij} - \bar{d}_j)^2} \tag{5}$$

and $\bar{d}_j$ is the mean of the j-th variable

$$\bar{d}_j = \frac{1}{n_{\mathrm{spec}}}\sum_{i=1}^{n_{\mathrm{spec}}} d_{ij} \tag{6}$$

Usually ratios 4 are displayed for all of the variables in the form of the spectrum (purity spectrum). The highest maximum in the first purity spectrum marks the first pure variable.

The determination of the second pure variable requires some additional considerations. All of the pure variables following the first must satisfy an additional constraint. They must have the highest ratio 4 and must be orthogonal to the all previously determined pure variables. Hence, the ratio 4 is multiplied by the determinant factor that is obtained in the following way. After the first variable has been found, then 2 × 2 matrices (**D**) are formed from the vector of the first pure variable placed always in the first row and the vectors of all other variables subsequently taking place in the second row. Then, cross products $\mathbf{D} \times \mathbf{D}^{\mathrm{T}}$ are formed, and the corresponding determinants are calculated. These determinants display similarity between the vector of the first pure variable and vectors of other variables. All variables similar to the first pure one will give small determinants reducing the values of ratio 4, while those more orthogonal will enhance the ratio 4. It should be stressed that prior to the calculations the spectra must be scaled to give equal statistical weights to all the variables. Also, an offset must be applied to diminish the problem of noisy variables, which might be serious when scaling.

Experimental Section

The water sample was prepared by passing tap water through activated charcoal and reverse osmosis filters. The water was then distilled and purified by an Ultrapure Water System (model GSR-200, Advantec, Japan). The resistance of the finally prepared water was greater than 18.1 MΩ cm^{-2}.

NIR spectra of water were measured from 1200 to 2500 nm at a 1 nm resolution by a Nicolet FTIR/NIR spectrometer (Magna series 760, Nicolet Instruments Corporation, Madison, WI) using a 1 mm quartz cell. The cell holder was connected to a water bath, and the sample temperature was controlled by circulating thermostated water. The temperature was measured by using a digital thermometer (TNA-20, Tasco Japan Co. Ltd., Osaka, Japan) dipped into the cell. This system guaranteed us a temperature control and stability of ±0.1 °C at 25 °C and ±0.2 °C at 80 °C. A total of 512 scans were co-added for measuring each spectrum. The sample was heated from 6 to 80 °C at 2 °C steps, yielding 38 sample spectra. The spectra were analyzed only in the 1300−1600 nm region. Some of the spectra were slightly below the wavelength axis, having a weak negative absorbance. To avoid possible calculation problems due to the appearance of negative spectral points, a numerical constant was added to move all of the spectra into the positive region. The algorithm for Simplisma is taken from ref 25. All of the calculations were carried out in Matlab 5.0 (MathWorks, Inc., Natick, MA).

Results

Figure 1 shows the NIR spectra of water measured over a temperature range of 6−76 °C with the increment of 10 °C.

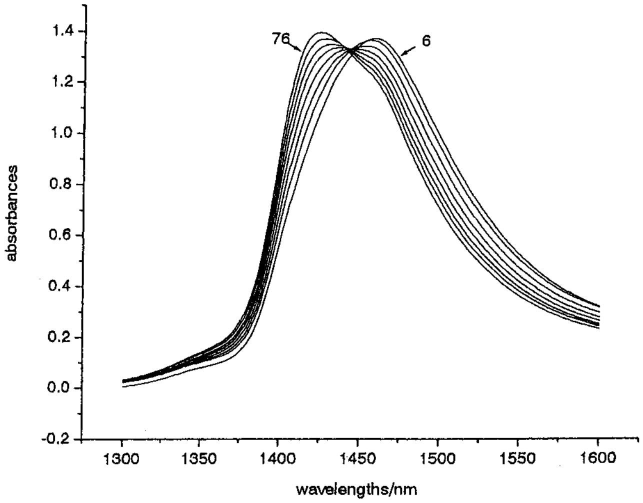

Figure 1. Eight experimental NIR spectra of pure water over a temperature range from 6 to 76 °C with the increment of 10 °C.

The bands in the region investigated arise from a combination of symmetric and antisymmetric O−H vibrations of water. It appears that the O−H peak shifts toward shorter wavelengths with increasing temperature. The first purity spectrum calculated by Simplisma is shown in Figure 2 (top). It demonstrates that the most unique variable in the spectral set is located just at its beginning. The shape of the top trace in Figure 2 excludes the possibility that identification of the very first variable in the spectral set (1300 nm) as the first pure variable is spurious. The trace is smooth and has reasonable shape, implying that the most average variable in the data set is the isosbestic point at 1445 nm the intensity of which does not change with temperature**.** Actually, Figure 1 reveals that a true isosbestic point does not exist in the investigated system of NIR spectra. However, if the first few spectra measured at the low temperatures are excluded from consideration, an isosbestic point emerges at 1445 nm. Throughout this paper, whenever the isosbestic point is referred to, one should keep in mind the above restriction concerning the isosbestic point.

The second purity spectrum reveals that 1539 nm is the second most specific variable (Figure 2, middle), representing an analyte that decreases with temperature. On the short wavelength side of the middle trace, all of the variables behave similarly to the one at 1300 nm, yielding very low intensity of the purity spectrum. Because the intensity changes are similar for all of the variables on the long wavelength side of the isosbestic point, the determinant factors have small values, and this is reflected in the disappearance of the short wavelength part of the curve from the top plot.

The third purity spectrum deserves particular attention (Figure 2, bottom). Namely, if the system is made up of only two species continuously converting one into the other, then all of the data can be explained by only two vectors aligned in **C** and **S**, while all other spectral and concentration vectors and the purity spectra that correspond to them should be noisy. Obviously, the third purity spectrum is not noiselike, and it merits the question whether it should be selected for further calculations. Its shape suggests selection, but its low intensity does not. Both shape and intensity are important factors for selection. The maximum of the third purity spectrum is 25 times weaker than the maximum of the second purity spectrum, implying that the third purity spectrum may represent noise or a very weak analyte. To resolve the ambiguity of the determination of the number of existing components, we have reproduced the experimental data choosing only the variables at 1300 and 1539 nm as the important ones. This means that intensity changes at 1300 and 1539 nm are taken as the columns of **C**, and then $\mathbf{S}^T$ is calculated according to eq 2. After that, the matrix of reproduced experimental data ($\mathbf{X}^{\mathrm{repr}}$) is obtained as $\mathbf{CS}^T$.

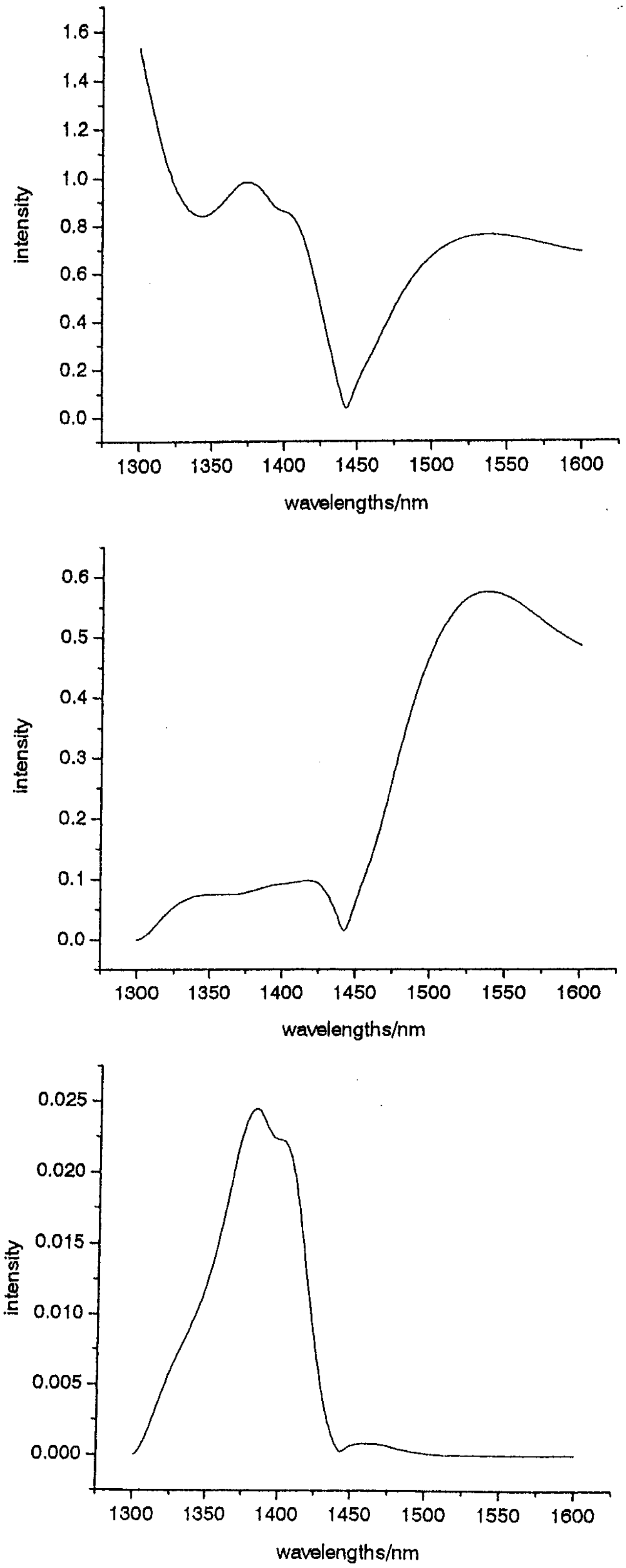

Figure 2. The first three purity spectra (from top to bottom) calculated by Simplisma.

The quality of the reproduction is illustrated for some of the reproduced spectra in Figure 3. Figure 4 shows matrix of residuals, **R**, calculated as $\mathbf{R} = \mathbf{X} - \mathbf{X}^{\mathrm{repr}}$. **R** is shown as a

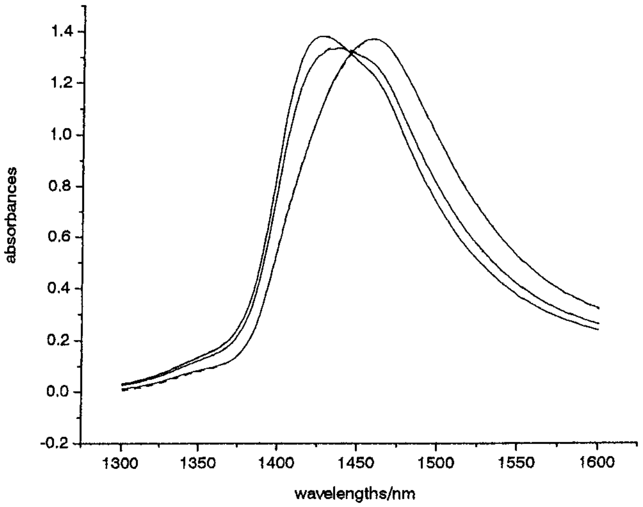

Figure 3. The reproduction of the spectra measured at 6, 50, and 80 °C. The lines mark original spectra, while the dots mark the spectra reproduced by the two-state approximation.

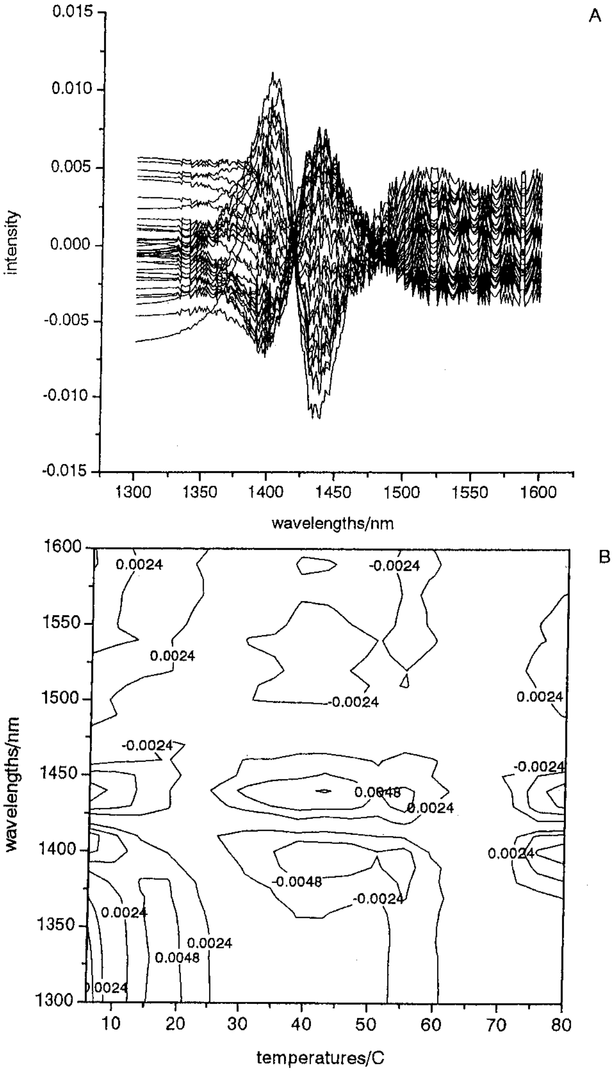

Figure 4. One-dimensional (A) representation of 38 residual spectra and two-dimensional (B) representation of residual matrix.

one-dimensional representation of all of the 38 residual spectra (Figure 4A), as well in a two-dimensional representation (Figure 4B), which enables better evaluation of the characteristics of given sample and wavelength region. It is noted in Figure 4A that the residuals are structured, having well-defined peaks at 1404, 1438, and 1516 nm and pronounced baseline fluctuations on the shorter wavelength side. Figure 4B reveals that errors in the reproduction of the experimental data are most pronounced for the temperature range 6−25 °C, becoming gradually smaller with the temperature increase. The spectral region around the isosbestic point seems to be reproduced with the highest error.

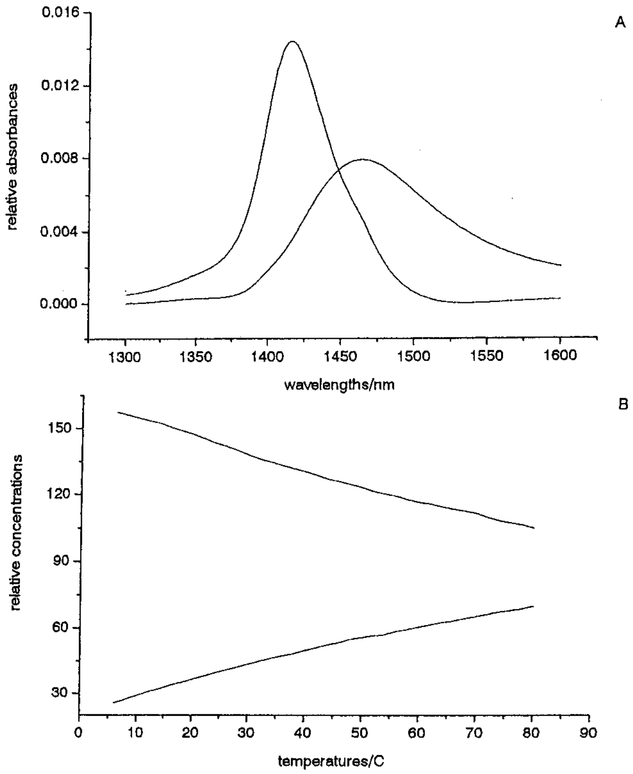

Figure 5. The first expressions of pure component spectra (A) and concentrations (B) calculated by Simplisma.

However, despite their spectra-like features, the reproduction errors are minor, as is evident from the ordinate in Figure 3. A more precise calculation shows that the total variation of the reproduced data in **R** (Figure 4) is only 0.4% of the total variation of the experimental data in Figure 1 (total variations for **R** and **X** are calculated as $\sum_i\sum_j r_{ij}$ and $\sum_i\sum_j x_{ij}$, where r_{ij} and x_{ij} are elements of **R** and **X**, respectively). Thus, we can conclude that the NIR spectra of water can be reproduced using only two vectors with the precision that more than 99% of the data are correctly reproduced. The residual of the approximation is not noise but contains structured data of which the overall influence on the spectral data is less than 0.4%, indicating that one can safely proceed to consider water as a two-component system.

Because the two-component option is chosen, the pure component spectra and concentrations are directly calculated by eqs 2 and 3, respectively, and shown in Figure 5 A,B. Because the spectra are scaled for the calculations, the features in Figure 5 are only proportional to the real ones, and to obtain the real solutions, one must rescale these spectra and concentrations. A broad band located at 1467 nm represents the HB analyte, while a band at 1413 nm represents the NHB analyte.

So far, we have not made any assumption or used any a priori knowledge about the system under investigation. However, from this point, we are compelled to exploit the features of the isosbestic point for the sake of rescaling the spectra. There is no other way to scale the data because we do not have the pure component spectra and do not know the absorption coefficients of the analytes, thereby preventing us from estimating the real

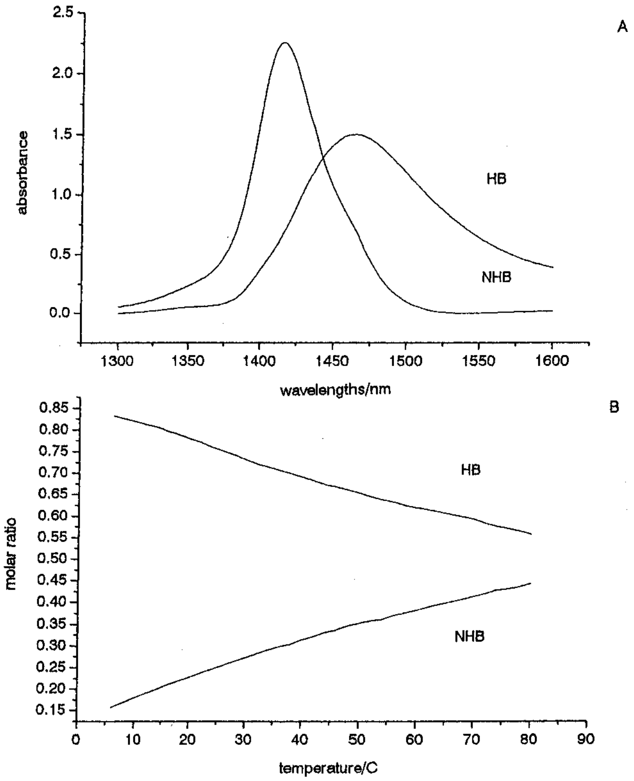

Figure 6. The spectra (A) and concentrations (B) of HB and NHB analytes after rescaling.

concentrations in any sample. Hence, we utilize the fact that at the isosbestic point both analytes must have the same absorption coefficients. The rigorous proof for this idea can be found in the literature by Verall and Senior[6] and Walrafen et al.[11] The correction factor needed to scale the spectra is found as[11,28]

$$f_j = x_i/s_{ji} \tag{7}$$

where x_i is the intensity of the experimental spectra at 1445 nm while s_{ji} is the intensity of the resolved spectrum at the same wavelength.

The final results for the pure component spectra are shown in Figure 6A. Figure 6B depicts the pure concentrations calculated by eq 3.

The Van't Hoff plot is calculated by using the molar ratios from Figure 6B and shown in Figure 7A where its linear fit is also given. Figure 7B compares our results with the results from the literature, most of which are concerned with Raman studies of water structure.[3,12,14−16,23,27] The best agreement between our results and the other results is found for the several Raman studies in which the scattering coefficients of HB and NHB species are assumed to be comparable, while the worst concurrence is seen with the Raman studies in which HB species are supposed to have a substantially larger scattering coefficient than NHB ones. The bands due to HB and NHB species are clearly seen in Raman spectra of water, but different methodologies employed to separate them led to diverse results that are seen in Figure 7B. The differences between our results and the results in the closest agreement with ours reveal that in our case the molar ratio of HB species is above the threshold foreseen by the percolation theory. The deviation of our experimental data from the linear fit shows that the two-state approximation gradually weakens with the temperature decrease. The slopes for all of the curves in Figure 7B seem to be comparable, meaning that enthalpy changes calculated from the data in Figure 7 are close to each other.

Discussion

Our results show that water can be considered a pseudo-two-component system. We have quantified variations of the analytes in the original and reproduced spectra and revealed that only 0.4% of the experimental data is left unexplained in the two-state approximation, which is in excellent agreement with the results reported by Libnau et al.[27,28] However, the residual data are not noisy and appear to be of greatest importance in the temperature range of 6−25 °C. Our efforts of extracting the realistic spectra of three components were fruitless because of the strong domination of NHB and HB species that completely mask the third, weak component. The extraction of the spectrum that is heavily overlapped with the spectra of two much more abundant species is almost impossible by the mathematical routine utilized here.

Our observations agree with previous work conducted by several research groups, most of which employed Raman spectroscopy. D'Arigo et al.[16] found in their Raman study that a two-state approximation gradually weakened as the temperature decreased below 20 °C. They concluded that it was in agreement with the percolation theory[18] and attributed the cause of breaking of the two-state model to ice fluctuations. Hare and Sorensen[22,23] reached largely the same conclusions as those by D'Arigo et al., but they assigned apparent breaking of the isosbestic point to the change in the nature of the scattering molecules. They also stated that a subtle relaxation of the rigid two-state model can successfully explain Raman spectra of water in the −33 to 80 °C region. Our results offer a sort of measure of the relaxation needed for the effectiveness of the two-state model.

An NIR study of H_2O−D_2O mixtures by Angell and Rodgers[19] suggested the existence of a broad band of H_2O near 1460 nm. They assigned it to spectral evidence for a network of slightly bent H bonds remaining almost constant during heating. Our results (Figures 2 (bottom) and 6) also suggest that, besides the two major analytes, an additional active species is probably present in the temperature range investigated. Its peak is located around 1440 nm, and its influence, as Simplisma shows, is quite weak. There is a difference of 20 nm between our result and that by Angell and Rodgers,[19] but the closeness of the isosbestic point and the fact that they approximated the position of the weak water band by utilizing glycerol−D_2O−H_2O solutions should be taken into consideration. The results reported here are obtained more straightforwardly.

Probably, we should emphasize one more point of accordance between our study and that by Angell and Rodgers.[19] They found that if some fraction of H bonds belonging to the network of bent bonds that is static in population is excluded from the total possible hydrogen bonds, the resulting Van't Hoff plot does not change noticeably compared with the simple two-state approach. We have, basically, found the same by omitting all of the spectral data resulting from non-NHB and -HB analytes and have found that the omission does not harm the original data significantly, thereby giving a solid base for the ΔH reported in Figure 7A.

On the basis of the above, the results obtained by SMCR are in line with the water structure given by Angell and Rodgers[19] and Hare and Sorensen,[22,23] meaning that the structure of water can be modeled by the two-component approximation based on spectroscopy evidence, but the continuous model approximation is more appropriate for hydrogen bonding. The hydrogen

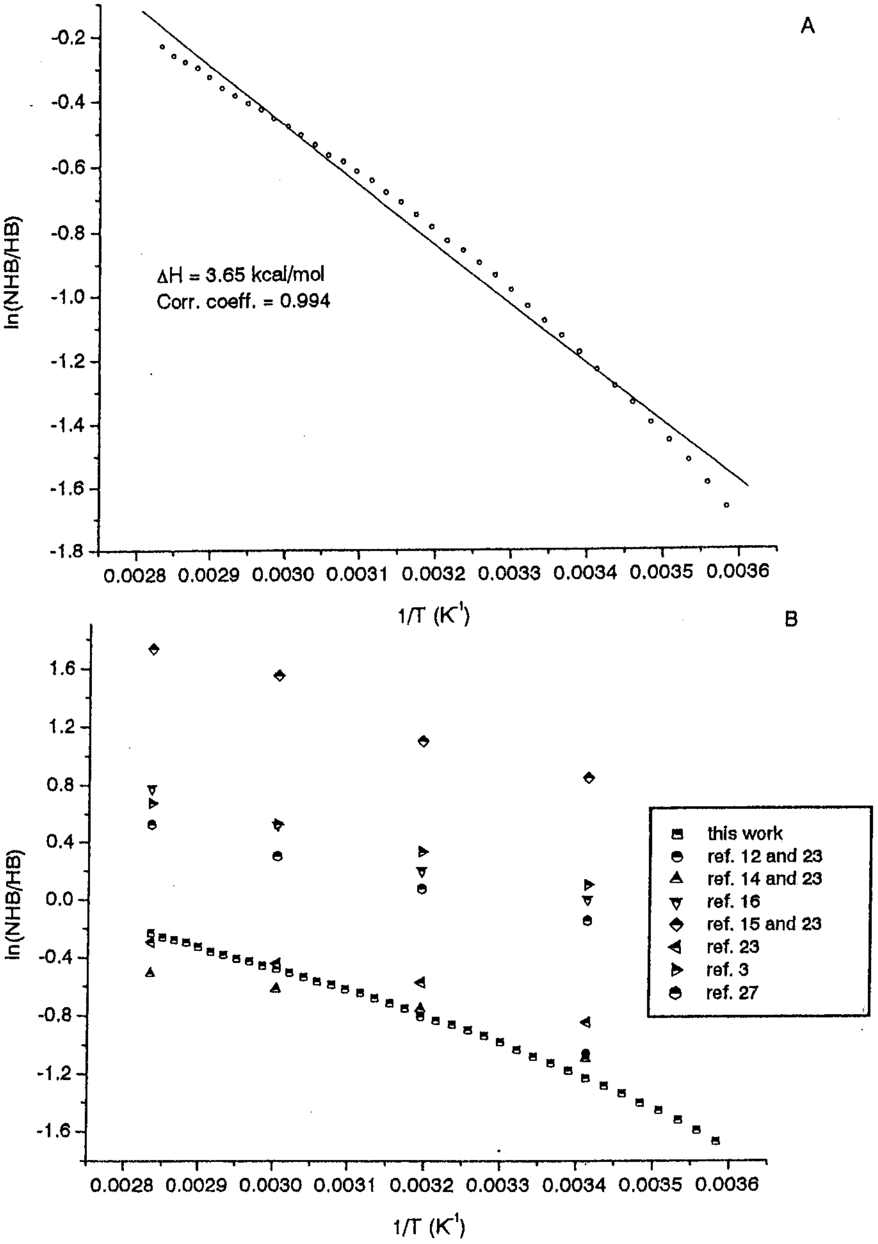

Figure 7. Van't Hoff plot (A) of the reaction of breaking one hydrogen bond in pure water and comparison with several other results (B) mostly obtained from Raman spectra.

bonds seem to be bent during heating, and the bending takes place uniformly because there is very weak evidence for the existence of more than one spectroscopically recognizable bent species. It is reasonable to assume that heating could induce the appearance of more than one NHB species, because the H−O···H angles could undergo several degrees of bending, each giving rise to its own spectral response. Our analysis reveals just weak indication that the NHB class of absorbers contains more than only one absorbing species. This can be seen in Figure 2, the third purity spectrum, and in the matrix of residuals, in which the errors of reproduction of experimental data are particularly discernible on the short wavelength side of the spectra.

It is here worth emphasizing that Libnau et al.[27,28] concluded that the lack of an isosbestic point was due to band broadening though they did not dismiss the shifts of peak positions. Their inference was based on the fact that residuals in their calculation (similar to those shown in Figure 4A) could have been generated by simulated band broadening. The effect of water bands broadening was discussed by Marechal,[29] while Nodland et al.[30] demonstrated the effect of band broadening on the curve resolution process. However, we support the above explanation on the basis of the indications of spectral and concentration characteristics of the residuals (Figure 4) and on the concordance with previously published studies although, numerically, broadening of Gaussian bands might yield results very similar to those discussed here.

Some novel theories of water structure stress the importance of H−O···H angles. A comprehensive experimental and theoretical study by Dougherty and Howard[31] proposed several types of hydrogen-bonded analytes differentiated by the H−O···H angles. They anticipate the existence of three water species in the temperature range covered by our study: pentagonal structure with an H−O···H angle of 108°, planar hexagonal with an H−O···H angle of 120°, and square structure in which squares of hydrogen-bonded water molecules are inferred with an H−O···H angle of 90°. According to Figure 3 in their work, all of the structures are constrained by the sum of the molar fractions to add up to 1. Measurable amounts of all of the above three structures were to be detected with smooth transitions among them, which means that none of the structures was favored. Our results definitely do not support this view. Even though the existence of the third spectroscopically active species does not seem to have any strong influence on the data, that is, the third analyte probably exists but has very weak intensity, absolute concentration profiles displayed in Figure 3 of ref 28 are not in accordance with the present study. What is, however, in agreement between the present study and that by Dougherty and Howard[31] is that the analyte assigned by them as pentagonal water vanishes at nearly 27 °C, as Figure 4B in the present study indicates to some extent.

On the other hand, Robinson's group suggested outer-neighbor interactions as one of the causes for the anomalies of water.[32,33] They stated that their model is "a mixture of ice-Ih- and ice-II-type bonding locally rearranging on picosecond scale". Increasing temperature causes a change in the distance of outer-neighbor O−O bonding from the ice-Ih type to the ice-II type that bends inner-neighbor H-bonds. The experimental evidences they reported mainly came from X-ray or neutron scattering measurements.[32,33] Strong support of their idea was presented by simulation studies in which their proposed water potential seems to be more efficient than potentials reported earlier. Vibrational spectroscopy, however, does not significantly assist their theory. Robinson et al.[32,33] strongly supported the two-state theory and quoted Raman studies by Walrafen et al.[10−13] who provided convincing evidences for the presence of an isosbestic point, which is a stable proof for the two-state system. However, the breakdown of the isosbestic point at the low temperatures is simply assigned to the experimental difficulties that are probably not serious problems, especially in the present study. It seems to us that the outer-neighbor interaction is difficult to prove by means of vibrational spectroscopy. The evidences for the outer-neighbor interactions obtained by the X-ray or neutron scattering measurements do not appear as clearly in the NIR spectra. The most important information that NIR spectra can offer is the number of analytes present and their respective concentrations. If this seems to be the ultimate goal of every spectral analysis, then one can safely conclude that for temperatures above 6 °C almost truthfully water spectra are made up from the spectra of two species. That itself provides too little information for backing (not only) the outer-neighbor theory. The additional problem is, of course, unambiguous presence of the very weak analyte, which does not violate the two-state model but the nature of which needs to be better understood.

Conclusion

The present study was undertaken with the aim of unravelling the NIR spectra of water by using advanced methods of analytical spectroscopy (Simplisma) and discussing the structure of liquid water. Without using any additional experimental data (only pure water spectra) and any prior knowledge about the spectral system under the investigation, we have identified the variables at 1300 and 1539 nm as the most representative, corresponding to the NHB and HB species, respectively. The spectra of NHB and HB species have been subsequently calculated on the basis of the two-state approximation. It has been shown that the two-state model approximation of water spectra is very satisfactory but the residuals that cover as small as 0.4% of the starting data are not noise. The most important features of the residuals are the peak at 1440 nm and significant response in the temperature range 6−25 °C, meaning that the NIR spectra of water are not a purely two-component system but a system that is very close. The spectra have been rescaled, and the enthalpy change of the single conversion from HB to NHB has been calculated. The result for ΔH is slightly higher than the ΔH reported by other groups based mainly upon the Raman spectra. The two-state approximation is found to gradually weaken as the temperature decreases. The overall evidences that we have gathered put toward the water structure suggested by Angell and Rodgers[19] and Hare and Sorensen[22,23] as quasi-lattice with broken bonds. Furthermore, the results obtained here bear important advantage that can be considered free from subjective and univariate assumptions and influences of errors arising from the complicated experimental setups.

References and Notes

(1) *Water, A Comprehensive Treatise*; Franks, F. Ed.; Plenum: New York, 1979; Vol. 1−6.
(2) Eisenberg, D.; Kauzmann, W. *The Structure and Properties of Water*; Oxford University Press: New York, 1969.
(3) Nemethy, G.; Sheraga, H. A. *J. Chem. Phys.* **1962**, *42*, 2563.
(4) Worley, J. D.; Klotz, I. M. *J. Chem. Phys.* **1965**, *45*, 2868.
(5) Hartman, K. A., Jr. *J. Phys. Chem.* **1966**, *70*, 270.
(6) Senior, W. A.; Verrall, R. E. *J. Phys. Chem.* **1969**, *73*, 4242.
(7) Wall, T. T.; Hornig, D. T. *J. Chem. Phys.* **1965**, *43*, 2079.
(8) Luck, W. A. P.; Ditter, W. *Z. Naturforsch., B* **1969**, *24*, 482.
(9) Luck, W. A. P.; Ditter, W. *J. Phys. Chem.* **1970**, *74*, 3687.
(10) Walrafen, G. E. *J. Chem. Phys.* **1970**, *52*, 4176.
(11) Walrafen, G. E.; Hokmabadi, M. S.; Yang, W. H. *J. Chem. Phys.* **1986**, *85*, 6964.
(12) Walrafen, G. E.; Fisher, M. R.; Hokmabadi, M. S.; Yang, W. H. *J. Chem. Phys.* **1986**, *85*, 6970.
(13) Walrafen, G. E.; Hokmabadi, M. S.; Yang, W. H. *J. Phys. Chem.* **1988**, *92*, 2433.
(14) Sherer, J. R.; Go, M. K.; Kint, S. *J. Phys. Chem.* **1974**, *78*, 1304.
(15) Bansil, R.; Wiafe-Akenten, J.; Taaffe, J. L. *J. Chem. Phys.* **1982**, *79*, 5863.
(16) D'Arigo, G.; Maisano, G.; Mallamace, F.; Migliardo, P.; Wanderlingh, F. *J. Chem. Phys.* **1981**, *75*, 4264.
(17) D'Arigo, G. *Nuovo Cimento B* **1981**, *61*, 123.
(18) Stanley, H. E.; Teixeira, J. *J. Chem. Phys.* **1980**, *73*, 3034.
(19) Angell, C. A.; Rodgers, V. *J. Chem. Phys.* **1984**, *80*, 6245.
(20) Green, J. L.; Lacey, A. R.; Sceats, M. G. *J. Chem. Phys.* **1987**, *86*, 1841.
(21) Ratcliffe, C. I.; Irish, D. E. *J. Phys. Chem.* **1982**, *86*, 4897.
(22) Hare, D. E.; Sorensen, C. D. *J. Chem. Phys.* **1990**, *93*, 6954.
(23) Hare, D. E.; Sorensen, C. D. *J. Chem. Phys.* **1990**, *93*, 26.
(24) Windig, W.; Guilment, G. *Anal. Chem.* **1991**, *63*, 1425.
(25) Windig, W.; Stevenson, D. A. *Anal. Chem.* **1992**, *64*, 2735.
(26) Windig, W. *Chemom. Intell. Lab. Syst.* **1997**, *36*, 3.
(27) Libnau, F. O.; Toft, J.; Christy, A. A.; Kvalheim, O. M. *J. Am. Chem. Soc.* **1994**, *116*, 8311.
(28) Libnau, F. O.; Kvalheim, O. M.; Christy, A. A.; Toft, J. *Vib. Spectrosc.* **1994**, *7*, 243.
(29) Marechal, Y. *J. Chem. Phys.* **1991**, *95*, 5565.
(30) Nodland, E.; Libnau, F. O.; Kvalheim, O. M. *Vib. Spectrosc.* **1996**, *12*, 163.
(31) Dougherty, R. C.; Howard, L. N. *J. Chem. Phys.* **1998**, *109*, 7379.
(32) Robinson, G. W.; Cho, C. H.; Urquidi, J. *J. Chem. Phys.* **1999**, *111*, 698.
(33) Cho, C. H.; Singh, S.; Robinson, G. W. *J. Chem. Phys.* **1997**, *107*, 7979.